

A multi-wavelength analysis of BL Her stars: Models versus Observations

S. Das¹, L. Molnár¹, S. M. Kanbur², M. Joyce¹, A. Bhardwaj³, H. P. Singh⁴,
M. Marconi³, V. Ripepi³ and R. Smolec⁵

¹Konkoly Observatory, Research Centre for Astronomy and Earth Sciences, Eötvös Loránd Research Network (ELKH), Konkoly-Thege Miklós út 15-17, H-1121, Budapest, Hungary

²Department of Physics, State University of New York Oswego, Oswego, NY 13126, USA

³INAF-Osservatorio Astronomico di Capodimonte, Salita Moiariello 16, 80131, Naples, Italy

⁴Department of Physics & Astrophysics, University of Delhi, Delhi 110007, India

⁵Nicolaus Copernicus Astronomical Center, Polish Academy of Sciences, Bartycka 18, PL-00-716 Warsaw, Poland

Abstract. We present new theoretical period–luminosity (PL) and period–radius (PR) relations at multiple wavelengths (Johnson–Cousins–Glass and *Gaia* passbands) for a fine grid of BL Hercules models computed using MESA-RSP. The non-linear models were computed for periods typical of BL Her stars, i.e. $1 \leq P(\text{days}) \leq 4$, covering a wide range of input parameters: metallicity ($-2.0 \text{ dex} \leq [\text{Fe}/\text{H}] \leq 0.0 \text{ dex}$), stellar mass ($0.5\text{--}0.8 M_{\odot}$), luminosity ($50\text{--}300 L_{\odot}$) and effective temperature (full extent of the instability strip; in steps of 50K). We investigate the impact of four sets of convection parameters on multi-wavelength properties. Most empirical relations match well with theoretical relations from the BL Her models computed using the four sets of convection parameters. No significant metallicity effects are seen in the PR relations. Another important result from our grid of BL Her models is that it supports combining PL relations of RR Lyrae and Type II Cepheids together as an alternative to classical Cepheids for the extragalactic distance scale calibration.

Keywords. stars: oscillations (including pulsations), stars: Population II, stars: variables: Cepheids, stars: low-mass

1. Introduction

Classical pulsators, in particular RR Lyrae stars, classical and Type II Cepheids are extremely important astrophysical objects; they are commonly used to estimate extragalactic distances, thanks to their well-defined period–luminosity (PL) relations, especially at longer wavelengths (for a review, see [Bhardwaj 2020](#)). However, although the effect of metallicity on the PL relations of RR Lyrae stars and classical Cepheids is minimised at near-infrared wavelengths, the precise calibration of PL-metallicity (PLZ) relations is one of the most important current topics of research in stellar variability studies (for example, see [Ripepi et al. 2021, 2022](#); [Breuval et al. 2022](#); [De Somma et al. 2022](#)). Type II Cepheids, on the other hand, are shown to exhibit little to no metallicity dependence on the PL relations ([Matsunaga et al. 2011](#); [Groenewegen and Jurkovic 2017](#); [Das et al. 2021](#)). Type II Cepheids are located in the classical instability strip of the Hertzsprung–Russell diagram. They have luminosities brighter than RR Lyrae but fainter than classical Cepheids. This makes them useful tracers, especially in regions with faint RR Lyrae and/or scarce classical Cepheids (for a review, see [Wallerstein 2002](#)).

Type II Cepheids are further subclassified on the basis of their pulsational periods ([Soszyński et al. 2018](#)) into BL Her stars ($1 \lesssim P(\text{days}) \lesssim 4$), W Vir stars ($4 \lesssim P(\text{days}) \lesssim 20$) and RV Tau stars ($P \gtrsim 20$ days). An additional class includes the peculiar W Vir (pW Vir) stars, which are brighter and bluer than the normal W Vir stars ([Soszyński et al. 2008](#)). In this study,

we analyse only the shortest-period Type II Cepheids, i.e., BL Her stars, from both theoretical and empirical points of view. This is because MESA-RSP (Paxton et al. 2019) can reliably model BL Her stars but not the longer-period Type II Cepheids (W Vir and RV Tau stars) owing to their highly non-adiabatic nature. As alluded to already, both empirical (Matsunaga et al. 2006, 2009, 2011; Groenewegen and Jurkovic 2017) and theoretical (Di Criscienzo et al. 2007; Das et al. 2021) studies provide evidence of largely negligible effects of metallicity on the PL relations of BL Her stars and Type II Cepheids, in general. However, recent results from Wielgórski et al. (2022) indicate a significant effect of metallicity on the PL relations of field Type II Cepheids at near-infrared wavelengths, albeit with the caveat that their sample size was rather small, containing only 23 Type II Cepheids. If confirmed with more observational data using high-resolution spectroscopy and multiband photometry, this discrepancy between cluster and field Type II Cepheids could potentially turn into an open problem.

In this study, we use the state-of-the-art radial stellar pulsation code MESA-RSP to compute a fine grid of BL Her models using the four sets of convection parameters, derive new theoretical PL, period–Wesenheit (PW) and period–radius (PR) relations at multiple wavelengths (Johnson–Cousins–Glass *UBVRIJHKLL'M* and *Gaia* *GG_{BP}GRP* bands) and thereby study the effects of metallicity and convection parameters on these relations. We also compare our theoretical results with empirical results of BL Her stars in the LMC from *Gaia* Data Release 3 (DR3; Ripepi et al. 2019) and from Groenewegen and Jurkovic (2017) using OGLE data.

2. Data and Methodology

The computation of BL Her models using MESA-RSP and the subsequent final selection of the models used for this analysis have been described in Das et al. (2021). In brief, the BL Her models were computed using MESA r11701, which uses the Kuhfuss (1986) theory of turbulent convection and the method of stellar pulsation as prescribed by Smolec and Moskalik (2008). The four sets of convection parameters are from Table 4 of Paxton et al. (2019), each with increasing complexities: set A corresponds to the simplest convection model, set B has radiative cooling added, set C included turbulent pressure and turbulent flux and set D has all of these effects added simultaneously.

We begin with the linear computations covering a wide range of input parameters: metallicity ($-2.0 \text{ dex} \leq [\text{Fe}/\text{H}] \leq 0.0 \text{ dex}$), stellar mass ($0.5\text{--}0.8 M_{\odot}$), luminosity ($50\text{--}300 L_{\odot}$) and effective temperature (full extent of the instability strip; in steps of 50K) using the four sets of convection parameters, resulting in a combination of 20,412 models per convection set over the entire range of input parameters. The linear stability analysis yields the linear periods and the growth rates of the models in different radial pulsation modes. This helps us estimate the red and blue edges of the instability strip as traced by the positive growth rates of the fundamental-mode BL Her pulsators (see Figure 1; Das et al. 2021). We proceed with the non-linear computations of the models with linear periods between 0.8 and 4.2 days. The non-linear integrations are computed over 4000 pulsation cycles each and only those models are accepted for the final analysis that have non-linear periods between 1 and 4 days and satisfy the condition of full-amplitude stable pulsations (the amplitude of radius variation δR , the pulsation period P , and the fractional growth of the kinetic energy per pulsation period Γ do not vary by more than 0.01 over the last 100 cycles of the 4000-cycle integrations; see Figure 2; Das et al. 2021). Models that did not converge within 4000 cycles were not included in this study. After these conditions are met, we finally have 3266 BL Her models computed using set A, 2260 models using set B, 2632 models using set C and 2122 models using set D.

The bolometric luminosities generated as output from the non-linear computations of MESA-RSP are converted into absolute bolometric magnitudes and also into absolute magnitudes M_{λ} in a given passband λ , using either pre-computed (for transformation into Johnson–Cousins–Glass bands using Lejeune et al. 1998) or user-provided (for transformation into *Gaia*

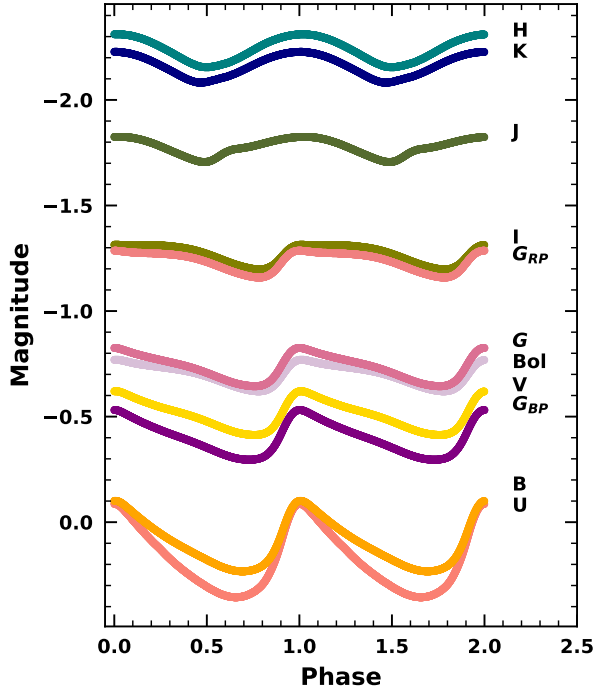


Figure 1. Example of multi-wavelength light curves for the BL Her model with input parameters, $Z = 0.00135$, $X = 0.74806$, $M = 0.6 M_{\odot}$, $L = 150 L_{\odot}$ and $T = 5500$ K, based on convective parameter set A.

passbands using the Packaged Model Grids from MESA Isochrones & Stellar Tracks, MIST[†]) bolometric correction tables. The bolometric correction tables are defined as a function of the stellar photosphere in terms of T_{eff} (K), $\log g$ (cm s^{-2}), and metallicity, $[M/H]$. An example of the light curves in both the bolometric magnitudes and in the different passbands for a BL Her model computed using convection parameter set A is presented in Figure 1.

The multi-wavelength theoretical light curves are fitted with the Fourier sine series (for an example, see Das et al. 2018) of the form,

$$m(x) = m_0 + \sum_{k=1}^N A_k \sin(2\pi kx + \phi_k), \quad (1)$$

where x is the pulsation phase, m_0 the mean magnitude and N the order of the fit ($N = 20$).

3. Period–luminosity relations

The mean magnitudes (M_{λ}) from the Fourier-fitted light curves of the BL Her models are used to obtain multi-wavelength PL relations of the mathematical form,

$$M_{\lambda} = a \log(P) + b \quad (2)$$

in a given band, λ . The multi-wavelength PL relations of the BL Her models computed using the four sets of convection parameters are summarised in Table 1 and compared using the standard t -test. In brief, we define a T statistic for the comparison of two linear regression

[†] <https://waps.cfa.harvard.edu/MIST/index.html>

Table 1. Comparison of the slopes of the PL and PW relations for BL Her stars of the mathematical form $M_\lambda = a \log(P) + b$. N is the total number of stars, T represents the observed value of the t -statistic, and $p(t)$ gives the probability of acceptance of the null hypothesis (equal slopes). The bold-faced entries indicate that the null hypothesis of the equivalent PL slopes can be rejected.

Band	Source	a	b	σ	N	Reference [‡]	Theoretical/ Empirical	Set A	Set B	(T , $p(t)$) w.r.t. Set C	Set D
Bolometric	Z_{all} (Set A)	-1.799±0.028	-0.181±0.01	0.253	3266	TW	Theoretical
Bolometric	Z_{all} (Set B)	-1.581±0.03	-0.181±0.01	0.231	2260	TW	Theoretical	(5.245,0.0)
Bolometric	Z_{all} (Set C)	-1.693±0.031	-0.094±0.011	0.256	2632	TW	Theoretical	(2.532,0.006)	(2.609,0.005)
Bolometric	Z_{all} (Set D)	-1.559±0.032	-0.103±0.011	0.246	2122	TW	Theoretical	(5.625,0.0)	(0.512,0.304)	(3.051,0.001)	...
Bolometric	LMC	-1.749±0.200	0.141±0.051	0.274	57(4)	G17	Empirical	(0.248,0.402)	(0.831,0.203)	(0.277,0.391)	(0.938,0.174)
U	Z_{all} (Set A)	-0.841±0.044	0.185±0.015	0.391	3266	TW	Theoretical
U	Z_{all} (Set B)	-0.596±0.046	0.215±0.015	0.353	2260	TW	Theoretical	(3.846,0.0)
U	Z_{all} (Set C)	-0.422±0.051	0.298±0.018	0.428	2632	TW	Theoretical	(6.219,0.0)	(2.512,0.006)
U	Z_{all} (Set D)	-0.369±0.053	0.309±0.018	0.409	2122	TW	Theoretical	(6.851,0.0)	(3.213,0.001)	(0.722,0.235)	...
B	Z_{all} (Set A)	-1.166±0.04	0.187±0.014	0.351	3266	TW	Theoretical
B	Z_{all} (Set B)	-0.896±0.041	0.209±0.013	0.311	2260	TW	Theoretical	(4.764,0.0)
B	Z_{all} (Set C)	-0.942±0.043	0.33±0.015	0.359	2632	TW	Theoretical	(3.843,0.0)	(0.791,0.214)
B	Z_{all} (Set D)	-0.805±0.044	0.324±0.015	0.339	2122	TW	Theoretical	(6.1,0.0)	(1.508,0.066)	(2.235,0.013)	...
V	Z_{all} (Set A)	-1.616±0.032	-0.14±0.011	0.284	3266	TW	Theoretical
V	Z_{all} (Set B)	-1.374±0.034	-0.134±0.011	0.256	2260	TW	Theoretical	(5.221,0.0)
V	Z_{all} (Set C)	-1.487±0.034	-0.031±0.012	0.288	2632	TW	Theoretical	(2.761,0.003)	(2.343,0.01)
V	Z_{all} (Set D)	-1.337±0.036	-0.043±0.012	0.275	2122	TW	Theoretical	(5.829,0.0)	(0.757,0.225)	(3.023,0.001)	...
I	Z_{all} (Set A)	-2.043±0.025	-0.592±0.008	0.219	3266	TW	Theoretical
I	Z_{all} (Set B)	-1.848±0.027	-0.599±0.009	0.203	2260	TW	Theoretical	(5.386,0.0)
I	Z_{all} (Set C)	-1.932±0.027	-0.534±0.009	0.226	2632	TW	Theoretical	(3.05,0.001)	(2.223,0.013)
I	Z_{all} (Set D)	-1.81±0.028	-0.545±0.01	0.218	2122	TW	Theoretical	(6.225,0.0)	(0.976,0.165)	(3.129,0.001)	...
J	Z_{all} (Set A)	-2.303±0.021	-0.914±0.007	0.186	3266	TW	Theoretical
J	Z_{all} (Set B)	-2.131±0.023	-0.928±0.008	0.177	2260	TW	Theoretical	(5.505,0.0)
J	Z_{all} (Set C)	-2.239±0.023	-0.877±0.008	0.19	2632	TW	Theoretical	(2.067,0.019)	(3.332,0.0)
J	Z_{all} (Set D)	-2.122±0.024	-0.89±0.008	0.187	2122	TW	Theoretical	(5.617,0.0)	(0.243,0.404)	(3.497,0.0)	...
J	LMC	-2.164±0.240	17.131±0.038 (@0.3) [*]	0.25	55	M09	Empirical	(0.577,0.282)	(0.137,0.446)	(0.311,0.378)	(0.174,0.431)
J	LMC	-2.294±0.153	15.375±0.113 (@1.0) [†]	0.202	55	B17	Empirical	(0.058,0.477)	(1.054,0.146)	(0.355,0.361)	(1.111,0.133)
H	Z_{all} (Set A)	-2.57±0.018	-1.17±0.006	0.157	3266	TW	Theoretical
H	Z_{all} (Set B)	-2.429±0.02	-1.192±0.007	0.154	2260	TW	Theoretical	(5.236,0.0)
H	Z_{all} (Set C)	-2.529±0.019	-1.162±0.007	0.16	2632	TW	Theoretical	(1.568,0.058)	(3.587,0.0)
H	Z_{all} (Set D)	-2.432±0.021	-1.175±0.007	0.162	2122	TW	Theoretical	(5.048,0.0)	(0.081,0.468)	(3.439,0.0)	...
H	LMC	-2.259±0.248	16.857±0.039 (@0.3) [*]	0.26	54	M09	Empirical	(1.251,0.106)	(0.683,0.247)	(1.086,0.139)	(0.695,0.244)
H	LMC	-2.088±0.214	15.218±0.163 (@1.0) [†]	0.296	52	B17	Empirical	(2.244,0.012)	(1.587,0.056)	(2.053,0.02)	(1.6,0.055)
K	Z_{all} (Set A)	-2.528±0.018	-1.124±0.006	0.16	3266	TW	Theoretical
K	Z_{all} (Set B)	-2.383±0.021	-1.144±0.007	0.157	2260	TW	Theoretical	(5.308,0.0)
K	Z_{all} (Set C)	-2.483±0.02	-1.112±0.007	0.164	2632	TW	Theoretical	(1.7,0.045)	(3.526,0.0)
K	Z_{all} (Set D)	-2.383±0.021	-1.125±0.007	0.165	2122	TW	Theoretical	(5.194,0.0)	(0.008,0.497)	(3.453,0.0)	...
K_s	LMC	-1.992±0.278	16.733±0.040 (@0.3) [*]	0.26	47	M09	Empirical	(1.924,0.027)	(1.402,0.081)	(1.762,0.039)	(1.402,0.081)
K_s	LMC	2.083±0.151	15.162±0.114 (@1.0) [†]	0.262	47	B17	Empirical	(2.87,0.002)	(1.93,0.027)	(2.576,0.005)	(1.93,0.027)
G	Z_{all} (Set A)	-1.76±0.029	-0.263±0.01	0.262	3266	TW	Theoretical
G	Z_{all} (Set B)	-1.531±0.031	-0.261±0.01	0.237	2260	TW	Theoretical	(5.352,0.0)
G	Z_{all} (Set C)	-1.63±0.032	-0.171±0.011	0.267	2632	TW	Theoretical	(2.996,0.003)	(2.231,0.026)
G	Z_{all} (Set D)	-1.49±0.033	-0.183±0.011	0.255	2122	TW	Theoretical	(6.095,0.0)	(0.895,0.371)	(3.049,0.002)	...
G	LMC	-1.248±0.149	18.549±0.043	0.159	61	Gaia DR3	Empirical	(3.373,0.001)	(1.86,0.063)	(2.507,0.012)	(1.586,0.113)
G_{BP}	Z_{all} (Set A)	-1.543±0.033	-0.077±0.011	0.293	3266	TW	Theoretical
G_{BP}	Z_{all} (Set B)	-1.296±0.034	-0.068±0.011	0.262	2260	TW	Theoretical	(5.193,0.0)
G_{BP}	Z_{all} (Set C)	-1.382±0.036	0.034±0.012	0.299	2632	TW	Theoretical	(3.33,0.001)	(1.731,0.084)
G_{BP}	Z_{all} (Set D)	-1.238±0.037	0.024±0.013	0.284	2122	TW	Theoretical	(6.178,0.0)	(1.151,0.25)	(2.804,0.005)	...
G_{BP}	LMC	-0.759±0.254	18.628±0.074	0.247	55	Gaia DR3	Empirical	(3.061,0.002)	(2.095,0.036)	(2.428,0.015)	(1.866,0.062)
G_{RP}	Z_{all} (Set A)	-2.015±0.025	-0.588±0.009	0.225	3266	TW	Theoretical
G_{RP}	Z_{all} (Set B)	-1.81±0.027	-0.594±0.009	0.209	2260	TW	Theoretical	(5.503,0.0)
G_{RP}	Z_{all} (Set C)	-1.909±0.028	-0.523±0.01	0.231	2632	TW	Theoretical	(2.819,0.005)	(2.565,0.01)
G_{RP}	Z_{all} (Set D)	-1.779±0.029	-0.536±0.01	0.223	2122	TW	Theoretical	(6.144,0.0)	(0.783,0.434)	(3.271,0.001)	...
G_{RP}	LMC	-1.782±0.216	18.041±0.065	0.219	56	Gaia DR3	Empirical	(1.072,0.284)	(0.129,0.898)	(0.583,0.56)	(0.014,0.989)
$W(G_{\text{BP}} - G_{\text{RP}})$	Z_{all} (Set A)	-2.656±0.018	-1.234±0.006	0.159	3266	TW	Theoretical
$W(G_{\text{BP}} - G_{\text{RP}})$	Z_{all} (Set B)	-2.507±0.021	-1.261±0.007	0.159	2260	TW	Theoretical	(5.432,0.0)
$W(G_{\text{BP}} - G_{\text{RP}})$	Z_{all} (Set C)	-2.633±0.019	-1.231±0.007	0.163	2632	TW	Theoretical	(0.887,0.375)	(4.412,0.0)
$W(G_{\text{BP}} - G_{\text{RP}})$	Z_{all} (Set D)	-2.517±0.021	-1.247±0.007	0.165	2122	TW	Theoretical	(4.98,0.0)	(0.341,0.733)	(3.994,0.0)	...
$W(G_{\text{BP}} - G_{\text{RP}})$	LMC	-2.362±0.205	17.312±0.061	0.206	58	Gaia DR3	Empirical	(1.429,0.153)	(0.704,0.482)	(1.316,0.188)	(0.752,0.452)
RR Lyrae PL relations compared with BL Her PL relations											
R	Z_{all}	-1.756±0.077	-0.114±0.014	0.196	226	M15	Theoretical	(1.19,0.117)	(1.485,0.069)	(0.208,0.418)	(1.882,0.03)
I	Z_{all}	-1.973±0.068	-0.415±0.013	0.175	226	M15	Theoretical	(0.966,0.167)	(1.709,0.044)	(0.561,0.287)	(2.217,0.013)
J	Z_{all}	-2.245±0.06	-0.778±0.011	0.155	226	M15	Theoretical	(0.902,0.184)	(1.769,0.039)	(0.098,0.461)	Stetbf(1.898,0.029)
H	Z_{all}	-2.206±0.118	-1.043±0.022	0.302	226	M15	Theoretical	(3.056,0.001)	(1.867,0.031)	(2.708,0.003)	(1.889,0.03)
K	Z_{all}	-2.514±0.057	-1.11±0.011	0.147	226	M15	Theoretical	(0.24,0.405)	(2.149,0.016)	(0.507,0.306)	(2.149,0.016)

[‡] TW = This work; M09 = Matsunaga et al. (2009); M15 = Marconi et al. (2015); B17 = Bhardwaj et al. (2017); G17 = Groenewegen and Jurkovic (2017)

^{*} Zero point at $\log(P) = 0.3$

[†] Zero point at $\log(P) = 1.0$

slopes, \hat{W} , with sample sizes, n and m , as follows:

$$T = \frac{\hat{W}_n - \hat{W}_m}{\sqrt{\text{Var}(\hat{W}_n) + \text{Var}(\hat{W}_m)}}, \quad (3)$$

where $\text{Var}(\hat{W})$ is the variance of the slope. The null hypothesis of equivalent slopes is rejected if $T > t_{\alpha/2, \nu}$ or the probability of the observed value of the T statistic is $p < 0.05$ where $t_{\alpha/2, \nu}$ is the critical value under the two-tailed t -distribution for the 95% confidence limit ($\alpha=0.05$) and degrees of freedom, $\nu = n + m - 4$.

From Table 1 we find that the BL Her models computed using sets B and D (with radiative cooling) exhibit statistically similar PL slopes at most wavelengths. In addition, although there

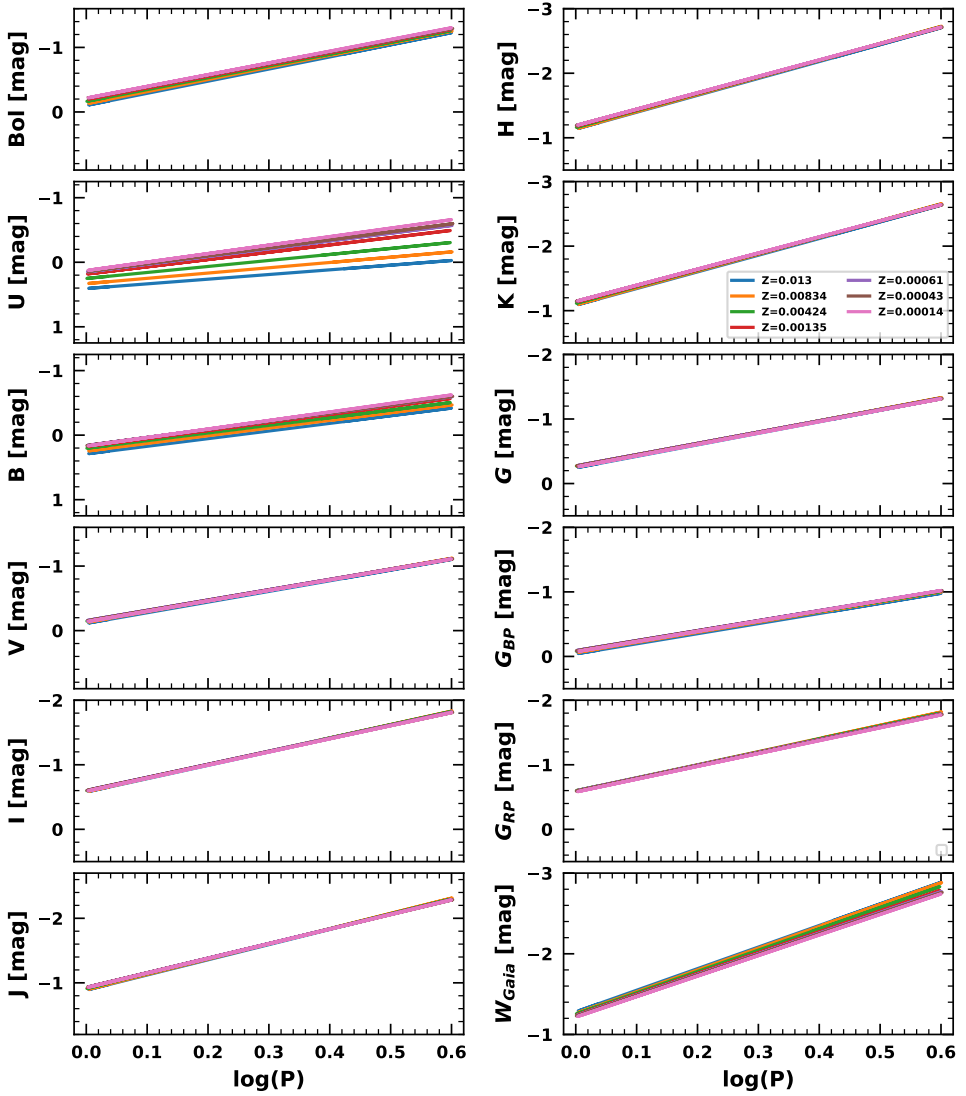


Figure 2. PL relations of the BL Her models with different chemical compositions at different wavelengths for the convective parameter set A. The y-axis scale is same (2.5 mag) in each panel to facilitate a relative comparison. The other convection parameter sets (B, C and D) show similar PL relations as a function of metallicity and wavelength.

exist differences in the PL slopes of the BL Her models computed using different convection parameters, the empirical PL slopes of BL Her stars in the LMC seem to match well with the theoretical PL slopes at most wavelengths. However, for a few particular cases ($HK_S GG_{BP}$), the empirical PL slopes of BL Her stars in the LMC seem to match better with the theoretical PL slopes obtained using models with radiative cooling. Note here that the *Gaia* apparent magnitudes used to obtain the empirical PL relations have not been corrected for extinction; however, to account for uncertainties arising from extinction, we also obtain empirical PW relations using Wesenheit magnitudes as defined by [Ripepi et al. \(2019\)](#) for *Gaia* DR3. We find the empirical PW slope of the BL Her stars in the LMC using *Gaia* DR3 for calibration to

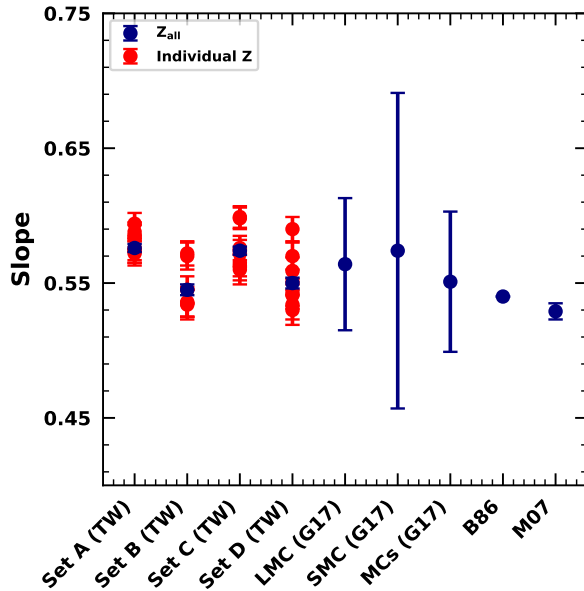


Figure 3. Comparison of the slopes of the PR relations for the BL Her stars obtained from this work (TW), using four different convective parameter sets, with those obtained from the literature. The red dots refer to the slopes of the PR relations obtained for the different chemical compositions individually, while the blue dots refer to the results obtained from considering the entire range of chemical compositions ($Z = 0.00014$ to $Z = 0.013$) combined. G17, B86 and M07 refer to [Groenewegen and Jurkovic \(2017\)](#), [Burki and Meylan \(1986\)](#) and [Marconi and Di Criscienzo \(2007\)](#), respectively.

be statistically similar to the theoretical PW slopes computed using the four sets of convection parameters.

The variation in the theoretical PL and PW relations obtained from the BL Her models as a function of metallicity is presented in Figure 2. We find strong effects of metallicity on the theoretical PL relations in the U and B bands, possibly because of increased sensitivity of bolometric corrections to metallicity at wavelengths shorter than the V band ([Gray 2005](#); [Kudritzki et al. 2008](#)). In the other bands, the theoretical PL relations exhibit little to no metallicity dependence; this is consistent with empirical PL relations from [Matsunaga et al. \(2006, 2009, 2011\)](#) and [Groenewegen and Jurkovic \(2017\)](#). An interesting result to note is the small but significant effect of metallicity on the theoretical PW relations using the *Gaia* passbands, although there seems to be no effect of metallicity on the individual *Gaia* passbands. We will probe into the possible reasons of this metallicity dependence in a future paper (Das et al., in prep.).

In addition, we also compare the PL relations obtained for the BL Her models with those from the recent grid of RR Lyrae models from [Marconi et al. \(2015\)](#) in the $RIJK_s$ bands. From the lowest panel of Table 1, we find the PL slopes of the RR Lyrae models to be statistically similar in the $RIJK_s$ bands to the BL Her models computed without radiative cooling (sets A and C). This equivalence of the PL relations from RR Lyrae and BL Her models is in agreement with empirical evidence from [Majaess \(2010\)](#), [Bhardwaj et al. \(2017\)](#) and [Braga et al. \(2020\)](#) and with previous theoretical analysis (for example, see [Di Criscienzo et al. 2007](#); [Marconi and Di Criscienzo 2007](#)) and supports the claim that it could be useful to obtain common PL relations from RR Lyrae and Type II Cepheids as an alternative to classical Cepheids for the calibration of the extragalactic distance scale.

4. Period–radius relations

We derive theoretical PR relations for the BL Her models of the mathematical form,

$$\log(R/R_{\odot}) = \alpha \log(P) + \beta, \quad (4)$$

where R is the mean radius of the BL Her model obtained by averaging the radius over a pulsation cycle.

A comparison of the slopes of the PR relations for the BL Her models computed using the four different convective parameter sets with those obtained from previous results from [Burki and Meylan \(1986\)](#), [Marconi and Di Criscienzo \(2007\)](#) and [Groenewegen and Jurkovic \(2017\)](#) is presented in Figure 3. We find that the BL Her models computed without radiative cooling (sets A and C) exhibit similar PR slopes while those computed using radiative cooling (sets B and D) have statistically similar PR slopes. The theoretical PR slopes of the BL Her models computed using the four sets of convection parameters are in broad agreement with the PR slopes from earlier empirical and theoretical results.

We also derive theoretical PRZ relations for the BL Her models of the form,

$$\log(R/R_{\odot}) = \alpha + \beta \log(P) + \gamma[\text{Fe}/\text{H}] \quad (5)$$

to test for the effects of metallicity on the PR relations. We find the following relations for set A, the simplest convection parameter set:

$$\begin{aligned} \log(R/R_{\odot}) = & (0.879 \pm 0.001) + (0.581 \pm 0.003) \log(P) \\ & - (0.006 \pm 0.001)[\text{Fe}/\text{H}] \quad (N = 3266; \sigma = 0.029), \end{aligned} \quad (6)$$

and for set D, the most complex convection parameter set:

$$\begin{aligned} \log(R/R_{\odot}) = & (0.886 \pm 0.002) + (0.554 \pm 0.004) \log(P) \\ & - (0.006 \pm 0.001)[\text{Fe}/\text{H}] \quad (N = 2122; \sigma = 0.029). \end{aligned} \quad (7)$$

The metallicity coefficient terms in Equations 6 and 7 indicate a weak dependence of the PR relations on metallicity, in agreement with previous empirical results from [Burki and Meylan \(1986\)](#) and [Groenewegen and Jurkovic \(2017\)](#).

5. Summary and Conclusions

We computed a very fine grid of BL Her models, the shortest period Type II Cepheids using MESA-RSP covering a wide range of input parameters: metallicity ($-2.0 \text{ dex} \leq [\text{Fe}/\text{H}] \leq 0.0 \text{ dex}$), stellar mass ($0.5\text{--}0.8 M_{\odot}$), luminosity ($50\text{--}300 L_{\odot}$) and effective temperature (full extent of the instability strip; in steps of 50K) with non-linear pulsational periods typical of BL Her stars, i.e., $1 \leq P(\text{days}) \leq 4$. The bolometric luminosities that result as an output of the non-linear computations were converted into absolute bolometric magnitudes and transformed into absolute magnitudes in the respective passbands (Johnson–Cousins–Glass *UBVRIJHKLL'M* and *Gaia* bands *GG_{BP}GRP*) using pre-computed or user-provided bolometric correction tables. The mean magnitudes obtained from Fourier fitting the light curves were then used to derive theoretical PL and PW relations.

As a function of different sets of convection parameters, the BL Her models computed using sets B and D (with radiative cooling) were found to exhibit statistically similar PL slopes at most wavelengths. While there exist differences among the theoretical PL relations of the BL Her models computed using the different sets of convection parameters, the empirical PL relations of BL Her stars in the LMC are in broad agreement with their theoretical counterparts, with some preference for models computed using radiative cooling especially in the *HK_sGG_{BP}* bands. The empirical PW slope of the BL Her stars in the LMC using *Gaia* DR3 is statistically similar to the theoretical PW slopes computed using the four sets of convection parameters. As a function of metallicity, there exists a strong effect of metallicity on the theoretical PL relations in the *U* and *B* bands, with weak to negligible effects of metallicity at

longer wavelengths, which is in agreement with earlier empirical results. We will probe the cause of the small but significant metallicity effect on the theoretical PW relations using the *Gaia* passbands in a future paper.

We also found a weak dependence of the PR relations on metallicity. In addition, the PL slopes of BL Her models computed without radiative cooling (sets A and C) using MESA-RSP are statistically similar to those for RR Lyrae models from [Marconi et al. \(2015\)](#) in the $RIJK_s$ bands, thereby supporting the claim that a common PL relation using RR Lyrae and Type II Cepheids could be used as an alternative to classical Cepheids for extragalactic distance scale calibrations. We also find the results from the MESA-RSP-computed grid of BL Her models to be in good agreement with previous theoretical predictions from [Di Criscienzo et al. \(2007\)](#); [Marconi and Di Criscienzo \(2007\)](#) for BL Her stars.

6. Acknowledgements

S. D. and L. M. acknowledge the KKP-137523 ‘SeismoLab’ Élvonal grant of the Hungarian Research, Development and Innovation Office (NKFIH). M. J. gratefully acknowledges funding from MATISSE: *Measuring Ages Through Isochrones, Seismology, and Stellar Evolution*, awarded through the European Commission’s Widening Fellowship. This project has received funding from the European Union’s Horizon 2020 research and innovation program.

References

- Bhardwaj, A., Macri, L. M., Rejkuba, M., et al. 2017, *AJ*, 153, 154
 Bhardwaj, A. 2020, *JAA*, 41, 23
 Braga, V. F., Bono, G., Fiorentino, G., et al. 2020, *A&A*, 644, A95
 Breuval, L., Riess, A. G., Kervella, P., Anderson, R. I., & Romaniello, M. 2022, *ApJ*, 939, 89
 Burki, G., & Meylan, G. 1986, *A&A*, 159, 261
 Das, S., Bhardwaj, A., Kanbur, S. M., Singh, H. P., & Marconi, M. 2018, *MNRAS*, 481, 2000
 Das, S., Kanbur, S. M., Smolec, R., et al. 2021, *MNRAS*, 501, 875
 De Somma, G., Marconi, M., Molinaro, R., et al. 2022, *ApJS*, 262, 25
 Di Criscienzo, M., Caputo, F., Marconi, M., & Cassisi, S. 2007, *A&A*, 471, 893
 Gray, D. F. 2005, *The Observation and Analysis of Stellar Photospheres*
 Groenewegen, M. A. T., & Jurkovic, M. I. 2017, *A&A*, 604, A29
 Kudritzki, R.-P., Urbaneja, M. A., Bresolin, F., et al. 2008, *ApJ*, 681, 269
 Kuhfuss, R. 1986, *A&A*, 160, 116
 Lejeune, T., Cuisinier, F., & Buser, R. 1998, *A&AS*, 130, 65
 Majaess, D. J. 2010, *JAVSO*, 38, 100
 Marconi, M., & Di Criscienzo, M. 2007, *A&A*, 467, 223
 Marconi, M., Coppola, G., Bono, G., et al. 2015, *ApJ*, 808, 50
 Matsunaga, N., Fukushi, H., Nakada, Y., et al. 2006, *MNRAS*, 370, 1979
 Matsunaga, N., Feast, M. W., & Menzies, J. W. 2009, *MNRAS*, 397, 933
 Matsunaga, N., Feast, M. W., & Soszyński, I. 2011, *MNRAS*, 413, 223
 Paxton, B., Smolec, R., Schwab, J., et al. 2019, *ApJS*, 243, 10
 Ripepi, V., Molinaro, R., Musella, I., et al. 2019, *A&A*, 625, A14
 Ripepi, V., Catanzaro, G., Molinaro, R., et al. 2021, *MNRAS*, 508, 4047
 Ripepi, V., Catanzaro, G., Clementini, G., et al. 2022, *A&A*, 659, A167
 Smolec, R., & Moskalik, P. 2008, *AcA*, 58, 193
 Soszyński, I., Udalski, A., Szymański, M. K., et al. 2008, *AcA*, 58, 293
 Soszyński, I., Udalski, A., Szymański, M. K., et al. 2018, *AcA*, 68, 89
 Wallerstein, G. 2002, *PASP*, 114, 689
 Wielgórski, P., Pietrzyński, G., Pilecki, B., et al. 2022, *ApJ*, 927, 89